

GADD34 induces cell death through inactivation of Akt following traumatic brain injury

JM Farook¹, J Shields², A Tawfik³, S Markand³, T Sen⁴, SB Smith³, D Brann¹, KM Dhandapani² and N Sen^{*1}

Neuronal cell death contributes significantly to the pathology of traumatic brain injury (TBI) irrespective of the mode or severity of the injury. Activation of a pro-survival protein, Akt, is known to be regulated by an E3 ligase TRAF6 through a process of ubiquitination-coupled phosphorylation at its T308 residue. Here we show that upregulation of a pro-apoptotic protein, GADD34, attenuates TRAF6-mediated Akt activation in a controlled cortical impact model of TBI in mice. TBI induces the expression of GADD34 by stimulating binding of a stress inducible transcription factor, ATF4, to the GADD34 promoter. GADD34 then binds with TRAF6 and prevents its interaction with Akt. This event leads to retention of Akt in the cytosol and prevents phosphorylation at the T308 position. Finally, *in vivo* depletion of GADD34 using a lentiviral knockdown approach leads to a rescue of Akt activation and markedly attenuates TBI-induced cell death.

Cell Death and Disease (2013) 4, e754; doi:10.1038/cddis.2013.280; published online 1 August 2013

Subject Category: Neuroscience

Traumatic brain injury (TBI) is a devastating neurological injury associated with significant morbidity and mortality.¹ TBI can be classified as mild, moderate and severe based on severity of the injury.^{2,3} However, irrespective of the severity, the most common symptom following TBI is cell death.⁴ One of the major features of TBI-induced cell death is an activation of NMDA receptors,^{5–7} which leads to a robust increase in oxidative⁸ and ER stress⁹ in cells. It is well established that upregulation of ER stress potentiates its effect through an increase in phosphorylation of PKR-like ER-associated kinase (PERK) protein, which subsequently phosphorylates eIF2 α to shut down global translation in cells.^{10,11} However, a few mRNA, such as the transcription factor ATF4, gain a selective advantage for translation under stress conditions. Intriguingly, recent work has further revealed that induction of oxidative stress in neurons leads to an increase of ATF4 in cells.¹²

Upon selective activation of ATF4, several stress-related genes such as *GADD34* are known to be upregulated. *GADD34* is member of a family of *GADD* genes that are induced by DNA damage, growth factor deprivation and other forms of cell stress.¹³ *GADD34* has been shown to bind the eukaryotic serine/threonine phosphatase protein phosphatase 1 to direct eIF-2 α dephosphorylation *in vitro*.^{14,15} Recent work suggests that the PERK is the major unfolded protein response-activated eIF-2 α kinase in mammalian cells.¹⁶ Phosphorylation of eIF-2 α by PERK or GCN2, a distinct eIF-2 α kinase that is activated by nutrient deprivation,¹⁷ promotes the expression of *GADD34*, which then assembles

an eIF-2 α phosphatase that functions in a negative feedback loop to reverse eIF-2 α phosphorylation and suppress the unfolded protein response.¹⁴ Further work has shown that expression of *GADD34* correlates with apoptosis induced by various signals, and its overexpression can initiate or enhance apoptosis.¹⁸

A significant body of work has shown that TBI-induced cell death is also correlated with activation of Akt.¹⁹ An important step of activation of Akt is its translocation from the cytosol to the plasma membrane, where it becomes activated in response to the stimulation of growth factor receptors at the cell surface.²⁰ Following growth factor-induced recruitment to the plasma membrane, Akt is phosphorylated at two conserved residues: (1) Thr308 within the active loop,^{21,22} and (2) Ser473 in the regulatory domain of Akt.^{23,24} The ubiquitin E3 ligase, TRAF6, can ubiquitinate Akt and promote its translocation to the plasma membrane, where it becomes phosphorylated at the T308 position. In cells lacking TRAF6, it was shown that ubiquitination, membrane localization, activation and signaling of Akt is impaired in response to treatment with growth factors.²⁵

In the present study, we report for the first time that augmentation of *GADD34* directly facilitates TBI-induced cell death in a controlled cortical impact model of TBI in mice. Oxidative or ER stress generated by TBI elicits a transcriptional increase in *GADD34*, enabling it to bind TRAF6 in competition with Akt. The binding of *GADD34* to TRAF6 prevents TRAF6-mediated ubiquitination of Akt and subsequently prevents membrane translocation and

¹Institute of Molecular Medicine and Genetics, Georgia Regents University, Augusta, GA, USA; ²Department of Neurosurgery, Georgia Regents University, Augusta, GA, USA; ³Department of Cellular Biology and Anatomy, Georgia Regents University, Augusta, GA, USA and ⁴Cancer Center, Georgia Regents University, Augusta, GA, USA

*Corresponding author: N Sen, Department of Neurology, Georgia Regents University, 1120 15th Street, CA 2018, Augusta, GA 30912, USA. Tel: +1 706 721 8185; Fax: +1 706 434 7097; E-mail: nsen@gru.edu

Keywords: Akt; *GADD34*; TBI; cell death; TRAF6

Abbreviations: *GADD34*, growth arrest and DNA damage-inducible protein 34; ATF4, activating transcription factor 4; Foxo3a, Forkhead box O3AA; BAD, Bcl-2-associated death promoter protein; PERK, Protein kinase-like endoplasmic reticulum kinase

Received 15.4.13; revised 21.6.13; accepted 28.6.13; Edited by A Verkhratsky

phosphorylation of Akt at T308 position. In intact mice, depletion of GADD34 in the cerebral cortex reduces TBI-induced cell death, suggesting that GADD34's binding to TRAF6 is critical for TBI-induced neurotoxicity. The competition between GADD34 and TRAF6 for Akt binding may reflect a regulatory system that maintains cellular homeostasis in response to stressors such as TBI.

Results

Inactivation of Akt is associated with cell death following TBI. To characterize the neurotoxic effects of TBI, we monitored cell death through the TUNEL assay following 12, 24, 48 and 72 h (Supplementary Figure 1b, Figure 1a) using pericontusional cortex (Supplementary Figure 1a) following TBI. We found that, the number of TUNEL-positive cells was augmented significantly in mice after 12 and 24 h post TBI compared with sham controls (Figure 1a). Moreover, consistent with findings by other investigators,^{26,27} we found that cell death was not further increased significantly after 24 h of TBI (Supplementary Figure 1b).

As activation of pro-survival proteins such as Akt is known to have a neuroprotective effect against various brain injuries including TBI, we monitored phosphorylation of Akt following TBI at 12, 24 and 48 h after TBI (Figure 1b and Supplementary Figure 1c). We found that phosphorylation of Akt at T308 residue was significantly decreased at 12 and 24 h after TBI, which was evidenced both by western blot (Figure 1b) and immunofluorescence microscopy (Figure 1c). We also found that phosphorylation of Akt at T308 was not further decreased at 24 h following TBI (Supplementary Figure 1c). However, phosphorylation of Akt at S473 was unaltered at 12 and 24 h after TBI (Supplementary Figure 1d).

It is known that activation of Akt leads to phosphorylation of various anti-apoptotic proteins such as Foxo3a at S256 residue,^{28,29} BAD at S136 residue^{30,31} and GSK3 β at S9 residue,^{32,33} which can minimize cell death. To determine whether the decrease in phosphorylation of Akt at the T308 position has any influence on phosphorylation levels of Foxo3a, Bad and GSK3 β , we performed western blot hybridization to monitor their phosphorylation levels. The results revealed that phosphorylation of GSK3 β , Foxo3a and Bad were decreased at 12 and 24 h after TBI (Figure 1d). This finding suggests that the decrease in phosphorylation of Akt at T308 is sufficient to reduce its catalytic activity. Phosphorylation of Akt depends on its membrane translocation. To determine whether TBI has any influence on membrane translocation of Akt, we measured the levels of Akt in both the cytosol and membrane fraction. We found that membrane translocation of Akt was decreased significantly at 12 h after TBI, and it was further decreased at 24 h post TBI (Figure 1e).

A decrease in TRAF6-mediated inactivation of Akt contributes to cell death following TBI. As TRAF6 is known to be a direct E3 ligase and essential for Akt ubiquitination, membrane translocation and phosphorylation, we examined the binding of TRAF6 and Akt in brain lysates following TBI. We found that the interaction between TRAF6

and Akt was markedly reduced at 12 and 24 h after TBI in mice (Figure 2a). Activation of NMDAR is considered a major cause for neuronal death after brain injury.⁵ In support of this contention, NMDAR antagonists were able to reduce cell death and improve outcome in animal models of TBI³⁴ and stroke.³⁵ To determine whether activation of NMDAR has any direct influence on Akt activation, we treated primary neurons *in vitro* with NMDA and found that NMDA significantly reduces interaction between TRAF6-Akt (Supplementary Figure 1e), phosphorylation of Akt (Supplementary Figure 1f) and ubiquitination of Akt (Figure 2b) that correlated with an increase in cell death (Figure 2c, compare bars 1 and 2). To establish whether the TRAF6-Akt cascade has any influence on NMDA-induced toxicity in primary neuronal cells, we depleted Akt in cells before treatment with NMDA. We found that NMDA-induced toxicity was increased significantly in cells depleted with Akt compared with cells treated with NMDA itself (Figure 2c, compare bars 3 and 4). To determine whether TRAF6 has any influence on NMDA-induced toxicity in cells, we overexpressed TRAF6 in control cells and in cells depleted with Akt. We found that cells overexpressing TRAF6 were able to restore NMDA-induced cell death to the extent of 85%. However, overexpression of TRAF6 in Akt-depleted cells was unable to restore NMDA-induced cell death (Figure 2c, compare bars 3 and 5). Collectively, these findings suggest that TRAF6 provides neuroprotection against NMDA-induced cell death in an Akt-dependent manner.

GADD34 interacts with TRAF6 following TBI. An important question is how is the interaction between TRAF6 and Akt reduced following TBI? One possibility is that TRAF6 levels are attenuated following TBI. However we did not see any change in the level of TRAF6 at 12 or 24 h after TBI (Supplementary Figure 2a). Another possibility is that TRAF6 may bind to other proteins in competition with Akt. To identify interacting proteins of TRAF6, co-immunoprecipitation coupled with mass-spectrometry analysis was performed on both sham and TBI mice samples. The results identified GADD34 as strongly interacting with TRAF6 in TBI samples. The binding was further confirmed by western blot hybridization (Figure 3a) and immunostaining procedure through confocal microscopy (Figure 3b). We also observed that TBI leads to an increase in the protein level of GADD34, which was evidenced by western blotting (Figure 3a, input level) and immunofluorescence staining (Figure 3c). To see whether GADD34 was regulated transcriptionally, we performed RT-PCR analysis of GADD34. We found that mRNA levels of GADD34 were upregulated following TBI (Figure 3d).

GADD34 is transcriptionally upregulated by ATF4 under TBI condition. GADD34 is an inducible protein whose expression is regulated by a transcription factor ATF4.¹⁰ Furthermore, both GADD34 and ATF4 can be induced by ER stress and oxidative stress. To confirm whether TBI leads to ER stress in the brain, we measured phospho-PERK and phospho-eIF2 α protein levels. The results revealed that levels for both phospho-PERK and phospho-eIF2 α were augmented at 12 and 24 h after TBI (Figure 4a). TBI also led to an increase in oxidative stress, as evidenced by

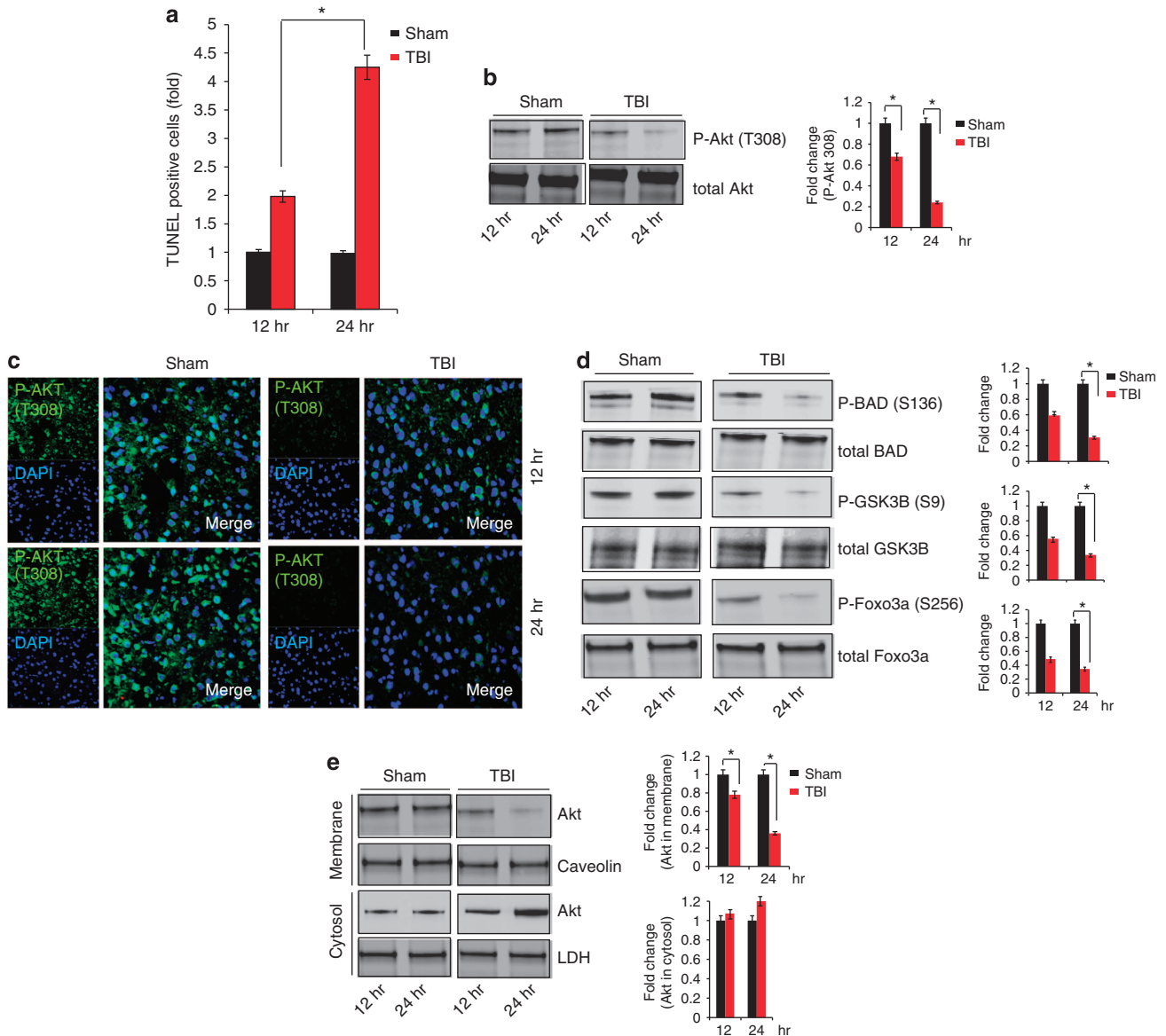


Figure 1 Inactivation of Akt is associated with cell death following TBI. (a) TUNEL staining was done to identify cell death at 12 and 24 h after TBI. Quantitative analysis shows that TUNEL staining was increased more than twofold after 24 h post TBI in the pericontusional cortex. (b and c) Phosphorylation of Akt (T308) was determined by western blot and immunofluorescent microscopy. Changes in phosphorylation status of Akt (P-Akt T308) was measured quantitatively. (d) Phosphorylation of downstream proteins of Akt, such as GSK3B, Foxo3a and BAD was determined by western blot analysis 12 and 24 h post TBI. (e) Membrane and cytosolic fraction of Akt was determined in the cortex at 12 and 24 h post Sham or TBI in mice. Level of both cytosolic and membrane Akt was determined at 12 and 24 h post TBI quantitatively. * $P < 0.01$, $n = 3$, one-way ANOVA, mean \pm S.E.M.

a significant increase in green fluorescence because of interaction between H2DCFDA with reactive oxygen species (Figure 4b). As ATF4 is known to be induced both by ER stress and oxidative stress, we examined protein levels of ATF4 by western blot analysis. We found that ATF4 levels were increased significantly at both 12 and 24 h after TBI (Figure 4c). To determine whether an upregulation of ATF4 directly contributes to an increase in GADD34, we performed chromatin immunoprecipitation assay to detect ATF4 binding to the GADD34 promoter. We found that binding of ATF4 to GADD34 promoter was increased more than twofold after both 12 and 24 h of TBI compared with sham control (Figure 4d).

To confirm that ER stress and oxidative stress can contribute directly to an increase in ATF4 levels, primary neurons in culture were pretreated with either an ER stress inhibitor (salubrinal) or an antioxidant (GSH) before treatment with the excitotoxic agent, NMDA. Treatment with NMDA led to an increase in both ATF4 and GADD34 levels, an effect that was blocked by pretreatment with either salubrinal or GSH (Figure 4e). These findings suggest that the TBI-induced increase in oxidative and ER stress likely causes upregulation of GADD34 via transcriptional activation of ATF4.

TBI-induced upregulation of GADD34 prevents TRAF6-mediated activation of Akt. An important question

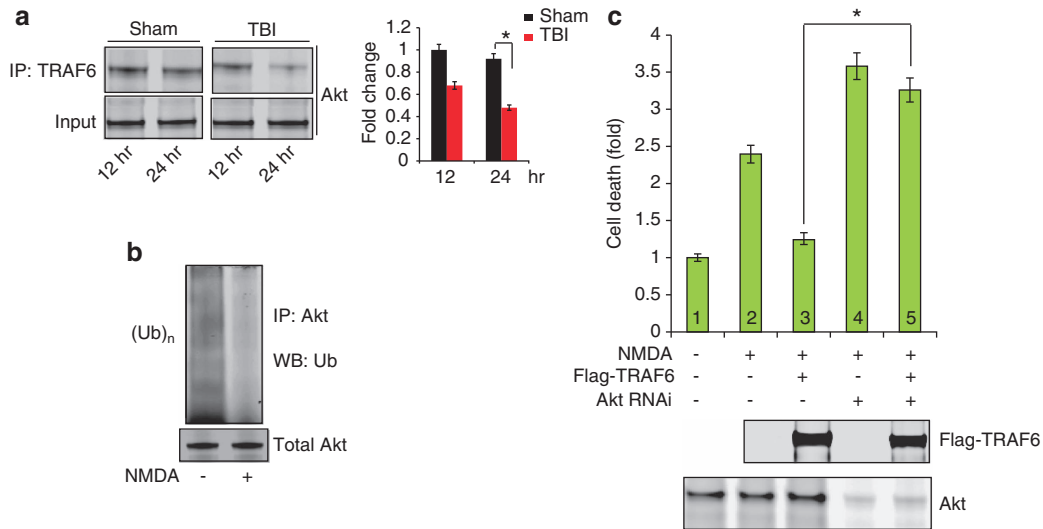


Figure 2 Effect of TRAF6 on Akt activation and cell death (a) Binding between TRAF6 and Akt was determined by co-immunoprecipitation assay at 12 and 24 h post TBI. (b) Ubiquitination assay of Akt was done using cell extracts with or without NMDA treatment. (c) Cell death was measured in primary neurons after overexpression of TRAF6 in the presence or absence of Akt inside cells. * $P < 0.01$, $n = 3$, one-way ANOVA, mean \pm S.E.M.

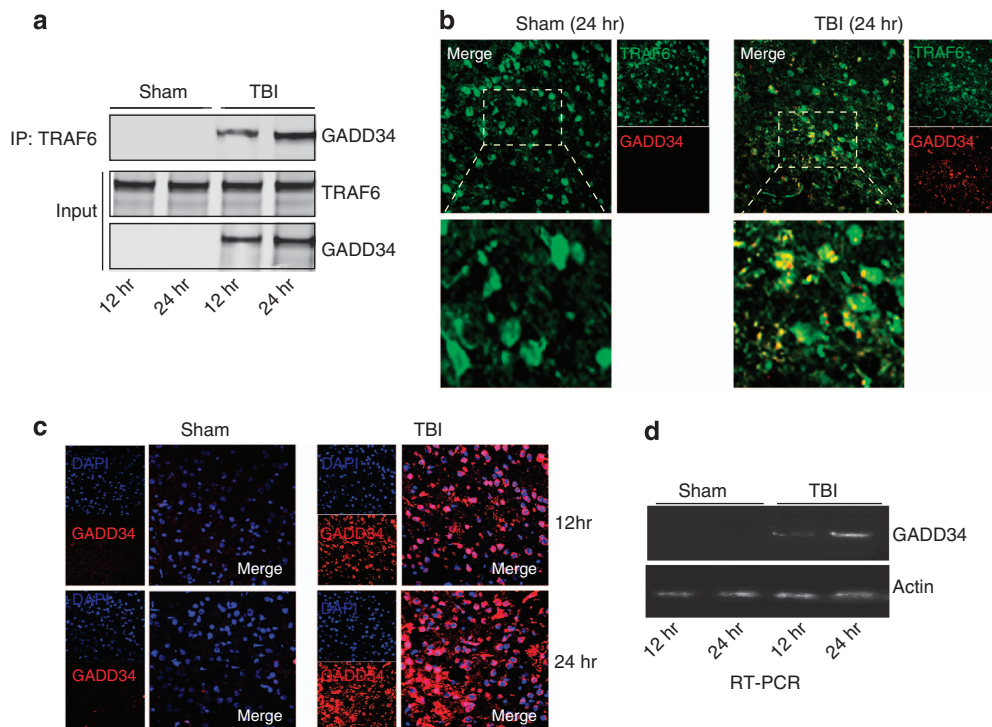


Figure 3 GADD34 interacts with TRAF6 following TBI (a and b) Interaction of GADD34 and TRAF6 was determined by both western blot analysis (a) and confocal microscopy (b) at 12 and 24 h post TBI. (c) Protein levels of GADD34 was monitored by immunofluorescent staining through confocal microscopy. (d) mRNA level of GADD34 was monitored by RT-PCR analysis at 12 and 24 h post TBI

is whether the interaction between GADD34 and TRAF6 has any influence on TRAF6-Akt interaction. To answer this question, we overexpressed GADD34 and TRAF6 in primary neurons, and determined the effect upon TRAF6-Akt interaction in the cells. The study revealed that GADD34 overexpression markedly diminished the binding of TRAF6 to Akt (Figure 5a). As the interaction between TRAF6 and Akt was attenuated by GADD34, we next examined whether

GADD34 elevation/overexpression affected phosphorylation and membrane translocation of Akt. As shown in Figures 5b and c, western blot analysis revealed that overexpression of GADD34 resulted in a significant decrease in the level of Akt phosphorylation (Figure 5b) and membrane translocation (Figure 5c) in cultured neurons.

To determine whether the interaction between GADD34-TRAF6 has any influence on cell death under treatment with

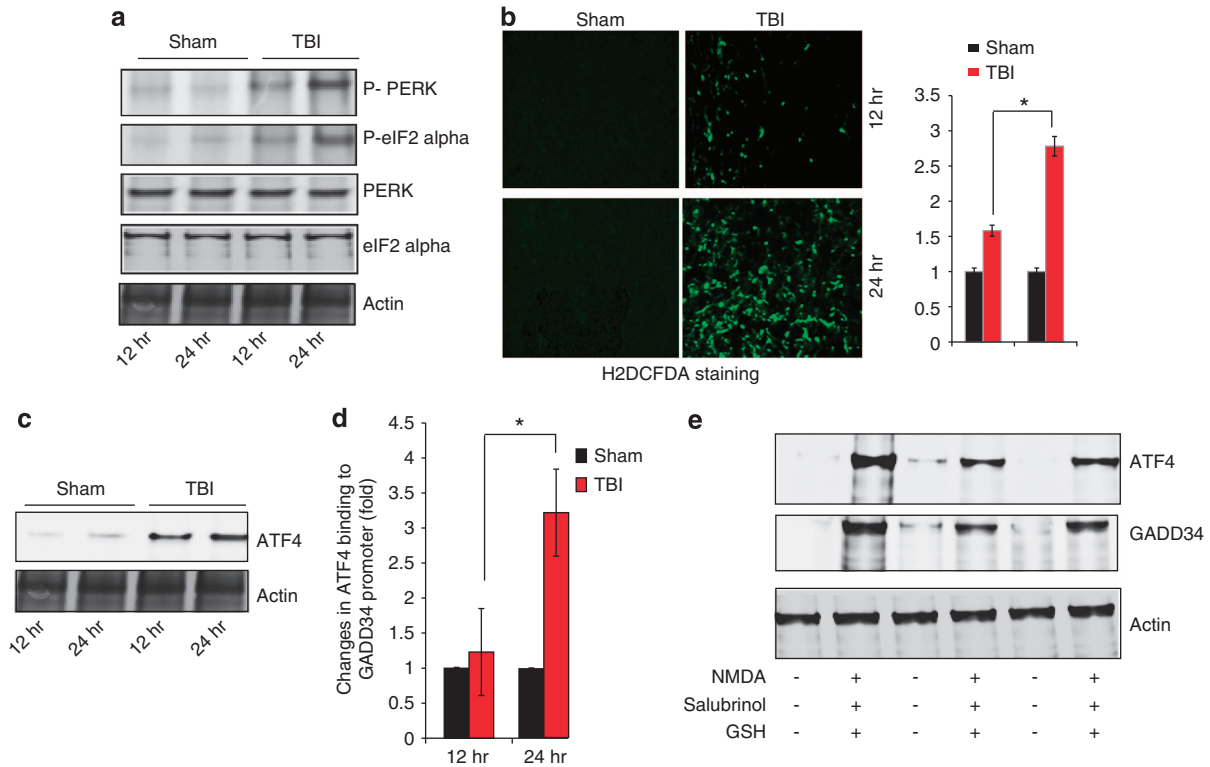


Figure 4 Both ER and oxidative stress regulates GADD34 levels following TBI. (a) Changes in the level of phosphorylation of PERK (P-PERK) and eIF2alpha (P-eIF2alpha) were determined through western blot analysis. (b) Changes in oxidative stress associated with TBI was measured by staining coronal sections of cortex with H2DCFDA dye. The intensity was quantified. (c) Western blot analysis to measure protein level of ATF4 following sham and TBI. (d) ATF4 binding to GADD34 promoter was determined by chromatin immunoprecipitation analysis. (e) Effect of GSH and salubrinal on the level of ATF4 and GADD34 that was induced by NMDA treatment in primary neuron. * $P < 0.01$, $n = 3$, one-way ANOVA, mean \pm S.E.M.

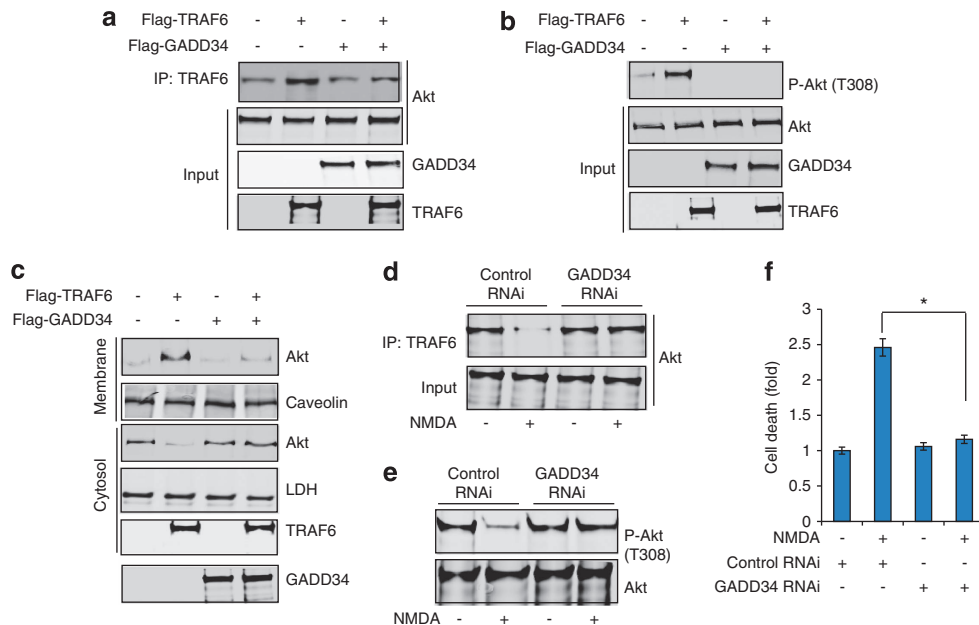


Figure 5 GADD34 causes inactivation of Akt at post TBI. (a) Overexpression of Flag-GADD34 causes a decrease in TRAF6-Akt interaction in primary cortical neurons. (b) Western blot analysis of phospho-Akt (T308) in primary neurons with or without overexpression of Flag-GADD34. (c) Western blot analysis of Akt in membrane or cytosol fractions with or without overexpression of Flag-GADD34. (d) Western blot analysis to detect interaction between TRAF6 and Akt after depletion of GADD34 in primary neurons. (e) Detection of phosphorylation status of Akt (T308) after doing RNAi knockdown of GADD34 in primary neurons. (f) Depletion of GADD34 causes a decrease in cell death in primary neurons after treatment with NMDA. * $P < 0.01$, $n = 3$, one-way ANOVA, mean \pm S.E.M.

a neurotoxic insult such as NMDA, we depleted GADD34 inside cells before inducing neurotoxicity elicited by NMDA. We observed that, cells lacking GADD34 restores interaction between TRAF6-Akt (Figure 5d), phosphorylation of Akt (Figure 5e) and attenuates NMDA-induced cell death (Figure 5f). These findings suggest that GADD34 directly influences Akt phosphorylation and cell death by competitively altering its interaction with TRAF6.

Depletion of GADD34 rescues TBI-induced Akt inactivation and cell death *in vivo*. As we have shown that upregulation of GADD34 enhances NMDA-induced cell death via inactivation of Akt in cultured neurons *in vitro*, we were interested to determine whether endogenous depletion of GADD34 would modulate TBI-induced cell death in mice. To deplete GADD34 levels in intact mice, we utilized a viral vector system that delivers RNAi particles of GADD34 into the cerebral cortex. Immunohistochemical staining revealed that lentiviral particles of control and GADD34 RNAi display similar levels of expression in the cerebral cortex (Figure 6a). We also monitored the expression level of GADD34 following sham and TBI conditions after administering lentiviral particles of GADD34 in brain. We found that GADD34 levels remain suppressed at 24 h either after sham or TBI (Figure 6b). Mice

overexpressing lentiviral particles of GADD34 RNAi exhibited a restored level of TRAF6-Akt interaction (Figure 6c) and phosphorylation of Akt (T308) (Figure 6d) at 24 h after TBI (e.g., more than 80% increased as compared with levels in mice overexpressing control RNAi). Of significant interest, depletion of endogenous GADD34 in mice brain significantly rescued TBI-induced cell death, as evidenced by a marked decrease in the number of TUNEL-positive cells (Figure 6e). Thus, downregulation of GADD34 in the cerebral cortex leads to selective diminution of TBI-induced neurotoxicity *in vivo*.

Discussion

In the current study, we demonstrate for the first time that TBI-induced oxidative and ER stress augments TRAF6-GADD34 binding, which competes with the interaction of TRAF6 with Akt. The GADD34 competition prevents TRAF6-mediated ubiquitination and activation of Akt, and thus blocks Akt neuroprotective activities in TBI (Figure 7). TRAF6 is known to ubiquitinate Akt following growth factor treatment in cells.²⁵ Additional work has shown that TRAF6-mediated ubiquitination of Akt also occurs in the liver and is important for glucose uptake. Interestingly, TRAF6 ubiquitination acts

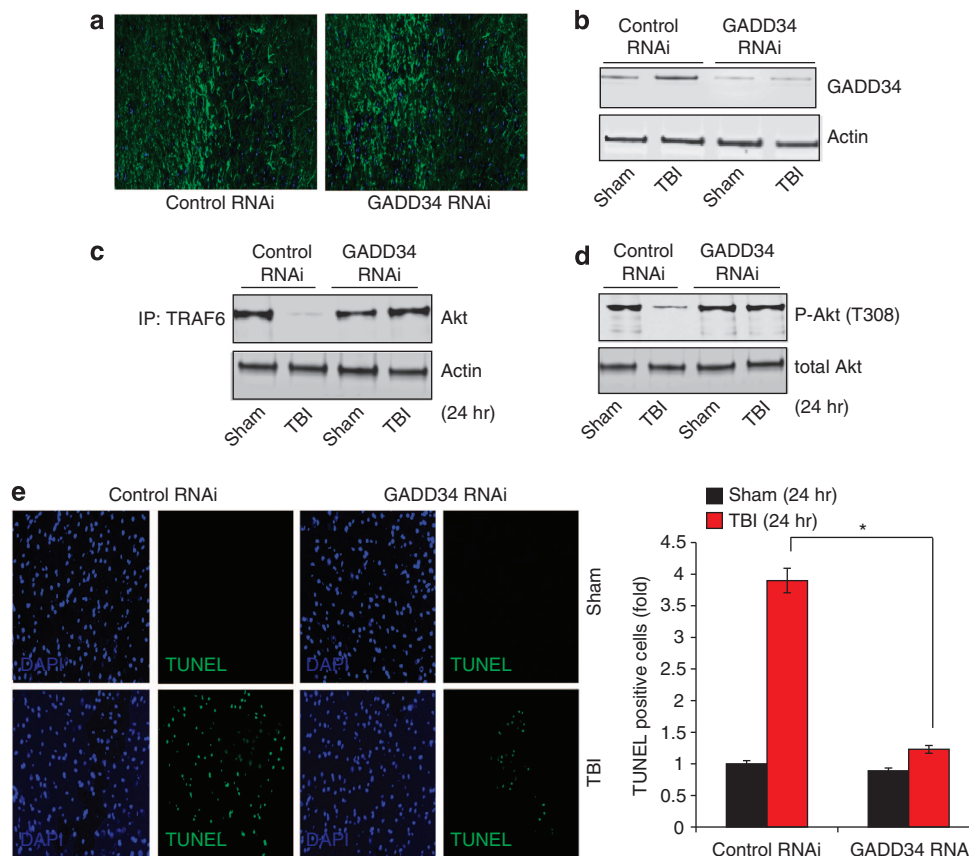


Figure 6 Depletion of GADD34 provides neuroprotection against TBI (a) Confocal microscopic analysis to determine expression of lentiviral RNAi particles in cortex. (b) Western blot analysis to detect levels of GADD34 in sham and TBI samples. (c) Western blot analysis to measure interaction between TRAF6 and Akt at 12 and 24 h post TBI in mice overexpressing either control or GADD34 RNAi particles in brain. (d) Analysis of phosphorylation of Akt (T308) at 12 and 24 h post TBI in mice overexpressing either control or GADD34 RNAi particles in brain. (e) Depletion of GADD34 decreases the number of TUNEL-positive neurons in cortex at 12 and 24 h after TBI. * $P < 0.01$, $n = 3$, one-way ANOVA, mean \pm S.E.M.

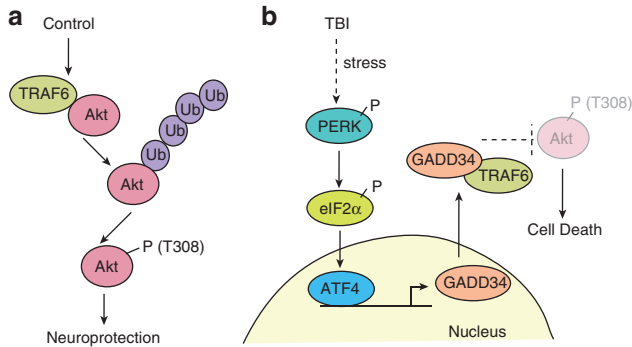


Figure 7 Schematic representation of how inactivation of Akt leads to cell death following TBI. (a) Under Sham condition, an E3 ligase TRAF6 binds with Akt and facilitates its ubiquitination and phosphorylation to provide neuroprotection. However, under TBI condition (b), ATF4 levels are augmented, which leads to an increase in the level of GADD34 in cells. GADD34 competitively interacts with TRAF6 and prevents interaction between TRAF6 and Akt, which leads to cell death.

through the K63-linked ubiquitination, but not the K48-linked ubiquitination. Thus, it does not affect the stability of Akt.²⁵ Secondly, Akt ubiquitination correlates well with Akt T308 phosphorylation and activation. Here, we have shown that TRAF6-mediated ubiquitination of Akt leads to phosphorylation at its T308 residue, which is important for its neuroprotection action against TBI. It is important to mention that TBI leads to a decrease in phosphorylation of Akt at the T308 position, whereas phosphorylation of Akt at the S473 residue remains unaltered. This is not so surprising, as it was previously shown that phosphorylation of these residues is independent from each other, and phosphorylation of each residue is sufficient to activate various downstream proteins in a context-dependent manner.^{25,36,37} In agreement with these results, we found that the decrease in phosphorylation of Akt at the T308 residue in neurons leads to a decrease in phosphorylation of various downstream proteins such as Foxo3a, GSK3 β and Bad, which are known to act as anti-apoptotic protein.

Previous work suggested that induction of GADD34 might allow the synthesis of pro-apoptotic proteins. Moreover, inhibition of eIF2 α phosphatases has been reported to reduce ER stress-induced apoptosis.^{38,39} To determine the influence of the interaction between GADD34-TRAF6 on phosphorylation status of eIF2 α , we depleted TRAF6 in primary neurons before treating with NMDA. The results revealed that the phosphorylation status of eIF2 α remains unaltered in cells lacking TRAF6, as compared with control RNAi-treated cells (Supplementary Figure 2b). This data provide evidence that GADD34 induces neurotoxicity independent of the eIF2 α pathway following TBI.

In conclusion, our study provides evidence that upregulation of GADD34 following TBI leads to cell death in an Akt-dependent manner. The molecular mechanism underlying this effect was shown to involve a competitive binding interaction of GADD34 with TRAF6, which prevents TRAF6-mediated activation of Akt in cells and augments neurotoxicity. Taken as a whole, our study provides new insight into the molecular mechanisms of cell death following TBI, which hopefully will facilitate development of new therapeutic

strategies to ameliorate cell death following TBI and lead to improved functional outcome.

Materials and Methods

Stereotaxic injection of lentivirus particles into intact mice.

Lentiviral particles of GADD34 RNAi were purchased from Santa Cruz (Santa Cruz, CA, USA) and administered in mouse brain according to the protocol described previously.⁴⁰ The Committee on Animal Use for Research and Education at Georgia Regents University approved all animal studies, in compliance with NIH guidelines. Adult male C57BL/6 mice (20–25 g; Charles River, Wilmington, MA, USA; Jackson Laboratory, Bar Harbor, ME, USA) were anesthetized with xylazine (8 mg/kg)/ketamine (60 mg/kg), and mounted on a stereotaxic frame (Stoelting, Wood Dale, IL, USA). The skull was exposed and 5.0 μ l (10^7 – 10^8 pfu/ml) of viral particles of GADD34 RNAi ($n=9$) protein was slowly injected into the cortex (anterior 0.5 mm, lateral 3.5 mm from bregma and ventral 1.0 mm relative to dura) over a period of 20 min using a 5.0 μ l Hamilton syringe, and the needle was left in place for an additional 5 min. Seven days after viral infection, depletion of GADD34 in coronal sections was detected by western blot analysis and immunohistochemistry with an anti-GADD34 antibody (1 : 200). On day 8, TBI was performed as described previously.^{41,42} After each injection, mice were placed in a thermoregulated chamber maintained at 31 ± 0.5 °C and returned to their cages after full recovery from anesthesia. The rectal temperatures were monitored and maintained at 37.0 ± 0.5 °C during the experimental procedure.

TBI procedures. The Committee on Animal Use for Research and Education at Georgia Regents University approved all animal studies, in compliance with NIH guidelines. The procedure was done based on a protocol described by Kimbler et al.⁴² Briefly, adult male C57BL/6 (Jackson Laboratory), mice were anesthetized with xylazine (8 mg/kg)/ketamine (60 mg/kg) and subjected to a sham injury or controlled cortical impact. Briefly, mice were placed in a stereotaxic frame (Amsci Instruments, Richmond, VA, USA) and a 3.5 mm craniotomy was made in the right parietal bone midway between bregma and lambda with the medial edge 12 mm lateral to the midline, leaving the dura intact. Mice were impacted at 4.5 m/s with a 20-ms dwell time and 12-mm depression using a 3-mm-diameter convex tip, mimicking a moderate TBI. Sham-operated mice underwent the identical surgical procedures, but were not impacted. The incision was closed with VetBond and mice were allowed to recover. Body temperature was maintained at 37 °C using a small animal temperature controller throughout all procedures (Kopf Instruments, Tujunga, CA, USA).

Immunohistochemistry. Deeply anesthetized mice were perfused with saline, followed by fixation with 4% paraformaldehyde in 0.1 M phosphate buffer (pH 7.4). Brains were post-fixed overnight in paraformaldehyde followed by cryoprotection with 30% sucrose (pH 7.4) until brains permeated. Serial coronal sections were prepared using a cryostat microtome (Leica, Wetzlar, Germany) and directly mounted onto glass slides. Sections were incubated at room temperature with 120% normal donkey serum in phosphate-buffered saline containing 0.4% Triton X-100 for 12 h, followed by incubation with the primary antibody (phosphor-Akt (T308), TRAF6, GADD34 (1 : 1000) cell signaling) overnight at 4 °C. Sections were then washed and incubated with the appropriate Alexa Fluor-tagged secondary antibody. Omission of primary antibody served as a negative control.

Confocal microscopy. Immunofluorescence was determined using a LSM 510 Meta confocal laser microscope (Carl Zeiss, Thornwood, NY, USA), as described previously.⁴¹ Cellular co-localization was determined in Z-stack mode using 63X oil immersion Neofluor objective (NA 12.3) with the image size set at 512×512 pixels. The following excitation lasers/emission filters settings were used for various chromophores: argon2 laser was used for Alexa Fluor 488, with excitation maxima at 490 nm and emission in the range 505–530 nm. A HeNe1 laser was used for Alexa Fluor 594 with excitation maxima at 543 nm and emission in the range 568–615 nm. Z-stacks (20 optical slices) were collected at optimal pinhole diameter at 12-bit pixel depth and converted into three-dimensional projection images using LSM 510 Meta imaging software (Carl Zeiss).

Measurement of reactive oxygen species. The determination of intracellular oxidant formation was based on the oxidation of the membrane-permeable probe 5-(6)-chloromethyl-2V,7V-dichlorodihydrofluorescein diacetate (CM-H2DCFDA) (Molecular Probes, Eugene, OR, USA) to yield an

intracellular-trapped fluorescent compound whose emissions at 530 nm can be captured when excited at 480 nm as described previously.⁴³ Brain segments were obtained from control and TBI mice, embedded in tissue freezing medium (TBS, Fisher, Pittsburg, PA, USA), frozen, cut into 30- μ m-thick sections and placed on glass slides. The sections were exposed to 10 μ M CM-H2 DCFDA in Krebs/HEPES buffer and slides were incubated in a light-protected humidified chamber at 37°C for 30 min. Fluorescence was then observed using Zeiss confocal microscope software (Carl Zeiss).

Measurement of NMDA-induced neurotoxicity in primary neurons. To activate NMDA receptors in neurons, 8- to 10-day-old cultures (DIC 8–10) were treated with Mg²⁺ + free Earle's balanced salt solution containing 300 μ M NMDA and 5 μ M glycine for 10 min as described previously.⁴⁰ Three days before NMDA receptor activation, cerebellar granule neurons were transfected with plasmids as follows: after preincubation of cells with neurobasal media (GIBCO BRL, Life Technologies, Grand Island, NY, USA), including B27 for 24 h from DIV 5, neurons were transfected with 1 μ g of RNAi of either control, TRAF6 or GADD34 (Santa Cruz) and a total of 3 μ g of varied combinations of plasmids using Lipofectamine 2000. Using confocal microscopy with a digital camera, we captured images of more than 20 fields per preparation, which were randomly chosen in a blind manner. GFP-positive neurons were tallied in each field and added together to determine the percentage of viable cells compared with control.

Three days before NMDA receptor activation, RNAi lentivirus was infected into cortical neurons. Viability of neurons was assayed 12 or 24 h after exposure to NMDA as follows: cells were washed with PBS and incubated in 1 μ g/ml propidium iodide for 10 min (dead cells are stained in red). After extensive washing to remove nonspecifically attached propidium iodide to cell debris by PBS, neurons were then fixed in 4% paraformaldehyde in PBS and stained with DAPI to visualize the total cell population. As the majority of neurons were infected, the ratio of propidium iodide-stained cells to DAPI-stained cells was employed to reflect toxicity.

Western blotting. Whole-tissue lysates were prepared from 3-mm coronal sections centered upon the site of impact. A 1-mm micropunch was collected from the pericontusional cortex or from the corresponding contralateral hemisphere as described previously.^{41,42} Tissue was placed in complete RIPA buffer, sonicated, and centrifuged for 120 min at 124 000 \times g at 4°C. Thirty micrograms of protein were resolved on a 4–20% SDS-polyacrylamide gel and transferred onto a polyvinylidene difluoride membrane. Blots were incubated overnight at 4°C in primary antibody Akt, phosphorylated-Akt (T308), phosphorylated-Akt (S473), GADD34, ATF4, phosphor-PERK, phosphor-eIF2 α (1:1000; Cell Signaling, Danvers, MA, USA) followed by a 2 h incubation with an Alexa Fluor-tagged secondary antibody at room temperature, per our laboratory. Blots were visualized using a Li-Cor Odyssey near-infrared imaging system and densitometry analysis was performed using Quantity One software (Bio-Rad, Foster City, CA, USA).

Statistical analysis. The effects of treatments were analyzed using a one-way analysis of variance (ANOVA) followed by Dunnett's *post hoc* test. Results are expressed as mean \pm S.E.M. A *P*-value <0.05 was considered to be statistically significant.

Conflict of Interest

The authors declare no conflict of interest.

Acknowledgements. JMF and NS were supported by the startup package provided by Georgia Regents University. JS and KMD were supported by NS065172 and NS075774 sponsored by NINDS. AT, SM and SBS were supported by EY012830S sponsored by NEI. DB was sponsored by NS050730 and NINDS.

- Nortje J, Menon DK. Traumatic brain injury: physiology, mechanisms, and outcome. *Curr Opin Neurol* 2004; **17**: 711–718.
- Saatman KE, Duhaime AC, Bullock R, Maas AI, Valadka A, Manley GT. Classification of traumatic brain injury for targeted therapies. *J Neurotrauma* 2008; **25**: 719–738.
- Maas AI, Stocchetti N, Bullock R. Moderate and severe traumatic brain injury in adults. *Lancet Neurol* 2008; **7**: 728–741.
- Raghupathi R, Graham DI, McIntosh TK. Apoptosis after traumatic brain injury. *J Neurotrauma* 2000; **17**: 927–938.
- Bieganski A, Fry PA, Paden CM, Alexandrovich A, Tsenter J, Shohami E. Dynamic changes in N-methyl-D-aspartate receptors after closed head injury in mice: Implications for treatment of neurological and cognitive deficits. *Proc Natl Acad Sci USA* 2004; **101**: 5117–5122.
- Dawson VL, Dawson TM. Deadly conversations: nuclear-mitochondrial cross-talk. *J Bioenerg Biomembr* 2004; **36**: 287–294.
- Takayasu M, Hara M, Yamauchi K, Yoshida M, Yoshida J. Transarticular screw fixation in the middle and lower cervical spine. Technical note. *J Neurosurg* 2003; **99**: 132–136.
- Reyes RC, Brennan AM, Shen Y, Baldwin Y, Swanson RA. Activation of neuronal NMDA receptors induces superoxide-mediated oxidative stress in neighboring neurons and astrocytes. *J Neurosci* 2012; **32**: 12973–12978.
- Sokka AL, Putkonen N, Mudo G, Pryazhnikov E, Reijonen S, Khirou L et al. Endoplasmic reticulum stress inhibition protects against excitotoxic neuronal injury in the rat brain. *J Neurosci* 2007; **27**: 901–908.
- Szegezdi E, Logue SE, Gorman AM, Samali A. Mediators of endoplasmic reticulum stress-induced apoptosis. *EMBO Reports* 2006; **7**: 880–885.
- Schroder M, Kaufman RJ. The mammalian unfolded protein response. *Ann Rev Biochem* 2005; **74**: 739–789.
- Lange PS, Chavez JC, Pinto JT, Coppola G, Sun CW, Townes TM et al. ATF4 is an oxidative stress-inducible, prodeath transcription factor in neurons *in vitro* and *in vivo*. *J Exp Med* 2008; **205**: 1227–1242.
- Zhan Q, Lord KA, Alamo Jr I, Hollander MC, Carrier F, Ron D et al. The gadd and MyD genes define a novel set of mammalian genes encoding acidic proteins that synergistically suppress cell growth. *Mol Cell Biol* 1994; **14**: 2361–2371.
- Connor JH, Weiser DC, Li S, Hallenbeck JM, Shenolikar S. Growth arrest and DNA damage-inducible protein GADD34 assembles a novel signaling complex containing protein phosphatase 1 and inhibitor 1. *Mol Cell Biol* 2001; **21**: 6841–6850.
- Noiva I, Zeng H, Harding HP, Ron D. Feedback inhibition of the unfolded protein response by GADD34-mediated dephosphorylation of eIF2 α . *J Cell Biol* 2001; **153**: 1011–1022.
- Harding HP, Zhang Y, Bertolotti A, Zeng H, Ron D. Perk is essential for translational regulation and cell survival during the unfolded protein response. *Mol Cell* 2000; **5**: 897–904.
- Sood R, Porter AC, Ma K, Quilliam LA, Wek RC. Pancreatic eukaryotic initiation factor-2 α kinase (PEK) homologues in humans, *Drosophila melanogaster* and *Caenorhabditis elegans* that mediate translational control in response to endoplasmic reticulum stress. *Biochem J* 2000; **346**(Pt 2): 281–293.
- Adler HT, Chinery R, Wu DY, Kussick SJ, Payne JM, Fornace Jr AJ et al. Leukemic HRX fusion proteins inhibit GADD34-induced apoptosis and associate with the GADD34 and hSNF5/INI1 proteins. *Mol Cell Biol* 1999; **19**: 7050–7060.
- Noshita N, Lewen A, Sugawara T, Chan PH. Akt phosphorylation and neuronal survival after traumatic brain injury in mice. *Neurobiol Disease* 2002; **9**: 294–304.
- Filippa N, Sable CL, Hemmings BA, Van Obberghen E. Effect of phosphoinositide-dependent kinase 1 on protein kinase B translocation and its subsequent activation. *Mol Cell Biol* 2000; **20**: 5712–5721.
- Alessi DR, Andjelkovic M, Caudwell B, Cron P, Morrice N, Cohen P et al. Mechanism of activation of protein kinase B by insulin and IGF-1. *EMBO J* 1996; **15**: 6541–6551.
- Alessi DR, James SR, Downes CP, Holmes AB, Gaffney PR, Reese CB et al. Characterization of a 3-phosphoinositide-dependent protein kinase which phosphorylates and activates protein kinase B α . *Curr Biol* 1997; **7**: 261–269.
- Feng J, Park J, Cron P, Hess D, Hemmings BA. Identification of a PKB/Akt hydrophobic motif Ser-473 kinase as DNA-dependent protein kinase. *J Biol Chem* 2004; **279**: 41189–41196.
- Sarbassov DD, Guertin DA, Ali SM, Sabatini DM. Phosphorylation and regulation of Akt/PKB by the rictor-mTOR complex. *Science* 2005; **307**: 1098–1101.
- Yang WL, Wang J, Chan CH, Lee SW, Campos AD, Lamothe B et al. The E3 ligase TRAF6 regulates Akt ubiquitination and activation. *Science* 2009; **325**: 1134–1138.
- Clark RSB, Chen M, Kochanek PM, Watkins SC, Jin KL, Draviam R et al. Detection of single- and double-strand DNA breaks after traumatic brain injury in rats: comparison of *in situ* labeling techniques using DNA polymerase I, the Klenow fragment of DNA polymerase I, and terminal deoxynucleotidyl transferase. *J Neurotrauma* 2001; **18**: 675–689.
- Chen SF, Tsai HJ, Hung TH, Chen CC, Lee CY, Wu CH et al. Salidroside improves behavioral and histological outcomes and reduces apoptosis via PI3K/Akt signaling after experimental traumatic brain injury. *PLoS One* 2012; **7**: e45763.
- Dijkers PF, Medema RH, Pals C, Banerji L, Thomas NS, Lam EW et al. Forkhead transcription factor FKHR-L1 modulates cytokine-dependent transcriptional regulation of p27(KIP1). *Mol Cell Biol* 2000; **20**: 9138–9148.
- Arden KC. FoxO: linking new signaling pathways. *Mol Cell* 2004; **14**: 416–418.
- Datta SR, Dudek H, Tao X, Masters S, Fu H, Gotoh Y et al. Akt phosphorylation of BAD couples survival signals to the cell-intrinsic death machinery. *Cell* 1997; **91**: 231–241.
- Del Peso L, Gonzalez-Garcia M, Page C, Herrera R, Nunez G. Interleukin-3-induced phosphorylation of BAD through the protein kinase Akt. *Science* 1997; **278**: 687–689.
- Srivastava AK, Pandey SK. Potential mechanism(s) involved in the regulation of glycogen synthesis by insulin. *Mol Cell Biochem* 1998; **182**: 135–141.

33. Cross DA, Alessi DR, Cohen P, Andjelkovich M, Hemmings BA. Inhibition of glycogen synthase kinase-3 by insulin mediated by protein kinase B. *Nature* 1995; **378**: 785–789.
34. Han RZ, Hu JJ, Weng YC, Li DF, Huang Y. NMDA receptor antagonist MK-801 reduces neuronal damage and preserves learning and memory in a rat model of traumatic brain injury. *Neurosci Bull* 2009; **25**: 367–375.
35. Gerriets T, Stolz E, Walberer M, Kaps M, Bachmann G, Fisher M *et al*. Neuroprotective effects of MK-801 in different rat stroke models for permanent middle cerebral artery occlusion: adverse effects of hypothalamic damage and strategies for its avoidance. *Stroke* 2003; **34**: 2234–2239.
36. Chakraborty A, Koldobskiy MA, Bello NT, Maxwell M, Potter JJ, Juluri KR *et al*. Inositol pyrophosphates inhibit Akt signaling, thereby regulating insulin sensitivity and weight gain. *Cell* 2010; **143**: 897–910.
37. Breuleux M, Klopfenstein M, Stephan C, Doughty CA, Barys L, Maira SM *et al*. Increased AKT S473 phosphorylation after mTORC1 inhibition is rictor dependent and does not predict tumor cell response to PI3K/mTOR inhibition. *Mol Cancer Ther* 2009; **8**: 742–753.
38. Boyce M, Bryant KF, Jousse C, Long K, Harding HP, Scheuner D *et al*. A selective inhibitor of eIF2alpha dephosphorylation protects cells from ER stress. *Science* 2005; **307**: 935–939.
39. Marciniak SJ, Yun CY, Oyadomari S, Novoa I, Zhang Y, Jungreis R *et al*. CHOP induces death by promoting protein synthesis and oxidation in the stressed endoplasmic reticulum. *Genes Dev* 2004; **18**: 3066–3077.
40. Sen N, Hara MR, Ahmad AS, Cascio MB, Kamiya A, Ehmsen JT *et al*. GOSPEL: a neuroprotective protein that binds to GAPDH upon S-nitrosylation. *Neuron* 2009; **63**: 81–91.
41. Zhang QG, Laird MD, Han D, Nguyen K, Scott E, Dong Y *et al*. Critical role of NADPH oxidase in neuronal oxidative damage and microglia activation following traumatic brain injury. *PLoS One* 2012; **7**: e34504.
42. Kimbler DE, Shields J, Yanasak N, Vender JR, Dhandapani KM. Activation of P2 × 7 promotes cerebral edema and neurological injury after traumatic brain injury in mice. *PLoS One* 2012; **7**: e41229.
43. Zhang X, Dong F, Ren J, Driscoll MJ, Culver B. High dietary fat induces NADPH oxidase-associated oxidative stress and inflammation in rat cerebral cortex. *Exp Neurol* 2005; **191**: 318–325.



Cell Death and Disease is an open-access journal published by Nature Publishing Group. This work is licensed under a Creative Commons Attribution-NonCommercial-NoDerivs 3.0 Unported License. To view a copy of this license, visit <http://creativecommons.org/licenses/by-nc-nd/3.0/>

Supplementary Information accompanies this paper on Cell Death and Disease website (<http://www.nature.com/cddis>)